

# Interstitial Fluid Flow Intensity Modulates Endothelial Sprouting in Restricted Src-Activated Cell Clusters During Capillary Morphogenesis

Rodrigo Hernández Vera, M.S.,<sup>1,2</sup> Elsa Genové, Ph.D.,<sup>1,2</sup> Lery Alvarez, B.S.,<sup>1</sup> Salvador Borrós, Ph.D.,<sup>2</sup> Roger Kamm, Ph.D.,<sup>1,3</sup> Douglas Lauffenburger, Ph.D.,<sup>3</sup> and Carlos E. Semino, Ph.D.,<sup>1-3</sup>

Development of tissues *in vitro* with dimensions larger than 150 to 200  $\mu\text{m}$  requires the presence of a functional vascular network. Therefore, we have studied capillary morphogenesis under controlled biological and biophysical conditions with the aim of promoting vascular structures in tissue constructs. We and others have previously demonstrated that physiological values of interstitial fluid flow normal to an endothelial monolayer in combination with vascular endothelial growth factor play a critical role during capillary morphogenesis by promoting cell sprouting. In the present work, we studied the effect that a range of interstitial flow velocities (0–50  $\mu\text{m}/\text{min}$ ) has in promoting the amount, length, and branching of developing sprouts during capillary morphogenesis. The number of capillary-like structures developed from human umbilical vein endothelial cell monolayers across the interstitial flow values tested was not significantly affected. Instead, the length and branching degree of the sprouts presented a significant maximum at flow velocities of 10 to 20  $\mu\text{m}/\text{min}$ . Moreover, at these same flow values, the phosphorylation level of Src also showed its peak. We discovered that capillary morphogenesis is restricted to patches of Src-activated cells (phosphorylated Src (pSrc)) at the monolayer, suggesting that the transduction pathway in charge of sensing the mechanical stimulus induced by flow is promoting predetermined mechanically sensitive areas (pSrc) to undergo capillary morphogenesis.

## Introduction

**A** MAJOR OBSTACLE for the development of three-dimensional tissue-engineered constructs is the ability to vascularize them. The most common scaffolds, made out of naturally occurring or synthetic materials, are deficient in promoting the formation of a vascular network essential to delivering nutrients and removing metabolic waste products. Tissue quality within cellular scaffolds declines dramatically from the surface to the interior, and cells located 200  $\mu\text{m}$  or further away from a blood supply become metabolically inactive or necrotic.<sup>1</sup> For this reason, we previously developed a sensitive and reliable system in which the chemical and biophysical parameters involved in the process of capillary morphogenesis could be easily assessed.<sup>2</sup> Using this device, we observed that human umbilical vein endothelial cell (HUVEC) monolayers engaged in capillary morphogenesis under the synergistic effect of low interstitial flows in combination with the presence of well-known pro-

angiogenic factors<sup>2</sup> (vascular endothelial growth factor (VEGF),<sup>3-10</sup> epithelial growth factor (EGF),<sup>3,11,12</sup> and basic fibroblast growth factor (FGFb)<sup>4,8,9,13</sup>). In particular, VEGF is involved in the main process of vasculogenesis during development, angiogenesis, tumor development, and vascular architecture maintenance in tissues and organs.<sup>3-10</sup> Two membrane receptors, KDR and Flt1, which contain the typical extracellular seven-immunoglobulin-like domains, a transmembrane domain, and a tyrosine kinase domain, recognize VEGF.<sup>14</sup> The recognition of VEGF by specific receptors in the endothelial cell membrane promotes tyrosine phosphorylation at their specific SH2 domains, inducing cell proliferation.<sup>15</sup>

Interstitial flow<sup>16-20</sup> (the movement of fluid through the extracellular matrix of a tissue) is present, to some extent, in all tissues and is responsible for the convection needed to transport<sup>21</sup> large proteins and other solutes through the interstitial space. In addition to this role, interstitial flow<sup>16-20</sup> also exerts a mechanical influence over interstitial cells directly,

<sup>1</sup>Center for Biomedical Engineering, Massachusetts Institute of Technology, Cambridge, Massachusetts.

<sup>2</sup>Department of Bioengineering, Tissue Engineering Division, Institut Químic de Sarrià, Universitat Ramon Llull, Barcelona, Spain.

<sup>3</sup>Biological Engineering Division, Massachusetts Institute of Technology, Cambridge, Massachusetts.

by the induction of shear stress, or indirectly, by imposing a strain and elastic stress to the extracellular matrix fibers to which the cells are attached via integrin receptors.<sup>18</sup> However, despite the known importance of interstitial fluid flow in tissue function, its influence over the cells is poorly understood. Although its role in blood and lymphatic capillary morphogenesis has been explored *in vitro*,<sup>2,17,20,22</sup> the specific mechanotransduction pathways involved in the process need to be further explored.

We previously showed that autocrine ligand activation of the epidermal growth factor receptor (EGFR) in combination with interstitial flow is critically involved in the morphogenic response of endothelial cells to VEGF.<sup>2</sup> In addition, we observed that, in our system, the EGFR was always activated (independently of interstitial flow) and that the use of EGFR pathway inhibitors (Galardin, AG1478, PD98059, and EGFR-blocking antibody) reduced the phosphorylation state of the receptor, correlating with an inhibition of capillary morphogenesis.<sup>2</sup> Interestingly, 5'-bromo-2'-deoxyuridine (BrdU) labeling identified dividing cells at the monolayer but not in any of the extending capillary-like structures. Moreover, sub-confluent cultures exposed to the EGFR inhibitors Galardin and AG1478 did not reduce BrdU incorporation into the monolayer, indicating that the EGFR-mediated morphogenesis is caused mainly by cell migration rather than proliferation. Testing of the proliferation activity under VEGF stimulation and different flow rates (corresponding to velocities of 0–160  $\mu\text{m}/\text{min}$ ) also revealed that values of approximately 10 to 20  $\mu\text{m}/\text{min}$ , previously described as physiologic,<sup>23</sup> are optimal for proliferation and reduce cell death.<sup>2</sup> Based on these results, we proposed a two-step model for experimental capillary morphogenesis in response to VEGF and interstitial fluid flow: monolayer maintenance by mitotic activity independent of EGFR signaling and migratory response mediated by autocrine activation of the EGFR pathway.<sup>2</sup> The proposed model suggests that cells undergoing cell division cannot migrate and will remain in the monolayer (e.g., in a less mechanically stressed zone), whereas non-proliferating cells can easily engage in migration and actively contribute to the development of capillary-like structures by undergoing morphogenesis. Although other groups have observed capillary morphogenesis in three-dimensional collagen and fibrin matrices before in the absence of interstitial flow, it is important to indicate that these experiments were conducted in the presence of phorbol 12-myristate 13-acetate, a potent activator of the protein kinase C, or sphingosine-1-phosphate, which enhances the matrix metalloproteinases and cell invasion.<sup>24–26</sup> Therefore, we have developed a system to eliminate the morphogenetic induction caused by the addition of phorbol 12-myristate 13-acetate or sphingosine-1-phosphate and to study in more detail the mechanical influence exerted by fluid flow.

With this body of evidence, we propose here that the mechanical effect of interstitial flow is promoting monolayer growth and, therefore, cell migration and extension of capillary-like structures. To test this hypothesis, in the present work, we studied in more detail the effect that a range of interstitial flow values (corresponding to velocities of 0–50  $\mu\text{m}/\text{min}$ ) have in promoting and maintaining capillary-like structures, as well as on the morphogenic responses such as the amount, length, and degree of branching of the developing sprouts. For this purpose, we developed a new

bioreactor made out of polydimethylsiloxane (PDMS), designed to work with interstitial flow, and allowing, at the same time, real-time microscopic monitoring of the capillary-like structures.

HUVEC monolayers cultured on collagen type I gels in the devices engaged in capillary morphogenesis under the synergistic effect of interstitial flow and VEGF, as expected. We observed that the amount of capillary-like structures developed from the endothelial monolayer across the interstitial flow values tested was not significantly affected. However, the length and branching degree of the capillary-like structures presented a significant maximum at flow values of 10 to 20  $\mu\text{m}/\text{min}$ . In other words, the number of capillary “initiation cases,” but not the length or branching, remained constant across the flow velocities tested. This suggests that the endothelial monolayer presents predetermined areas that could undergo capillary morphogenesis under the appropriated biomechanical conditions. In addition, the mechanical stimulus provided by flows corresponding to the maximum response value promoted capillary growth even while the number of events remains fixed. When we analyzed the phosphorylation state of Src<sup>27–30</sup> (a component of focal adhesion complexes) across the monolayer, we discovered that it presented a heterogeneous distribution, showing phosphorylated Src (pSrc) cell clusters surrounded by non-phosphorylated Src (non-pSrc) cells. The new capillary-like structures emerged always from pSrc clusters, indicating that predetermined Src-activated areas (pSrc) were the only restricted zones to undergo capillary morphogenesis and that the number of these was independent of interstitial flow. In conclusion, in our system the endothelial monolayer presents a predetermined distribution of potential capillary initiation clusters (pSrc) –(or mechanically sensitive zones) that, under adequate biomechanical stimulus, will engage in capillary morphogenesis, promoting cell migration out of the monolayer and therefore capillary extension and branching.

## Materials and Methods

### Materials

The following materials were purchased: PDMS (Sylgard 184 Silicone Elastomer Kit, Dow Corning, MI), endothelial semi-defined medium (EGM-2, CC-3162, Cambrex BioScience, Walkersville, MD,) collagen type I from rat tail (356236 BD, BD Biosciences, San Jose, CA), anti-BrdU mouse monoclonal antibody immunoglobulin (Ig)G (556028, BD Biosciences), 4',6-diamidino-2-phenylindole, dihydrochloride (DAPI; D-1306, Molecular Probes, OR), and tetramethyl rhodamine isothiocyanate (TRITC)-phalloidin (77418, Fluka, St. Louis, MO).

### Bioreactor fabrication

PDMS was prepared by mixing the base and curing reagent in an 8:1 ratio (v/v). Afterwards, the polymer mixture was placed inside a vacuum dryer to de-gas and then poured into the mold. The polymer was de-gassed once more, and then the mold was heated for 15 min at 120°C. Once the polymer was completely cured, the piece was peeled off, and the final assembly (Fig. 1A) was performed by putting the two halves together with Superflex Clear RTV (Henkel Loctite Corporation, Rocky Hill, CT).

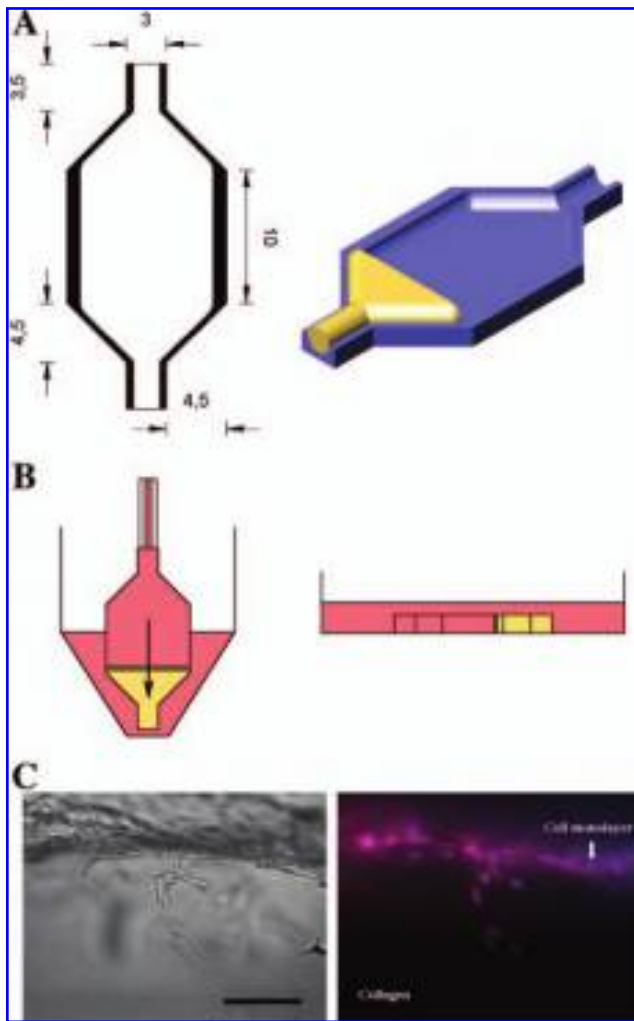


**FIG. 1.** Scheme of the new bioreactor: the collagen and capillary structure. (A) The bioreactor, made out of polydimethylsiloxane, was designed to work with interstitial flow and at the same time allow real-time microscopic monitoring of the capillary-like structures. The bioreactors, built and sterilized following the fabrication process described (see Materials and Methods), were loaded with a layer of collagen I and incubated for 30 min to allow gel formation. (B) The gels were then equilibrated with medium for 30 min before seeding primary derived human umbilical vein endothelial cells on top of them. Interstitial flow was applied using a syringe pump, and flow rates were set to obtain the desired mean flow velocities (2–50  $\mu\text{m}/\text{min}$ ) through the gel. Static controls were made by placing the bioreactors horizontally inside a Petri dish and covering them with medium. Left: longitudinal section of the device (dimensions shown are in mm). Right: isometric view of half the bioreactor showing the collagen gel. (C) Capillary-like structures formed. Bioreactors prepared following the procedure previously described (see Materials and Methods) were incubated overnight. Interstitial flow (11.5  $\mu\text{L}/\text{h}$ ) was then maintained for 48 h before the cells were fixed with 4% paraformaldehyde. Control experiments without flow were also performed (for details see above in B). The cells were stained with 4',6-diamidino-2-phenylindole, dihydrochloride (DAPI; to visualize nuclei) and tetramethyl rhodamine isothiocyanate-phalloidin to stain the actin fibers. Left: phase contrast image. Right: DAPI (blue) and actin staining (Red). Black bar in top-left panel represents 100  $\mu\text{m}$ . Color images available online at [www.liebertpub.com/ten](http://www.liebertpub.com/ten).

### Cell maintenance and culture in the bioreactors

Primary derived HUVECs (CC-2519, Cambrex BioScience), passages 3 to 9, were cultured in T-25 flasks previously coated with collagen type I (BD Bioscience, CA) using EGM-2 (CC-3162, Cambrex BioScience) without EGF or VEGF and containing 5% fetal bovine serum (FBS). Cells were maintained in a water-jacketed incubator at 37°C with 5% carbon dioxide ( $\text{CO}_2$ ) until they reached 80% confluence. The cells were finally washed with trypsin before being released from the plate with ethylenediaminetetraacetic acid (Versene, Gibco, NY).

The bioreactors were sterilized using 70% ethanol, and 100  $\mu\text{L}$  of collagen type I, prepared according to the manufacturer's recommendations, was injected into each of them. The devices were then placed in a water-jacketed incubator at 37°C with 5%  $\text{CO}_2$  for 30 min to allow gel formation. Next, the collagen gels were equilibrated with 100  $\mu\text{L}$  of EGM-2 with FGFb (1 ng/mL) and VEGF (10 ng/mL) for 30 min. Finally 100,000 cells were seeded on top of the gel and then incubated at 37°C with 5%  $\text{CO}_2$ .

### Application of interstitial flow

*Interstitial flow application through HUVEC monolayers in the bioreactors.* Endothelial cell monolayers were first cultured on top of the collagen gels as described above for 1 or 16 h according to the experiment, and flow was applied by using a syringe pump (55–2222, Harvard Apparatus, Holliston, MA). Flow rates were adjusted to obtain the desired mean flow velocities (2–50  $\mu\text{m}/\text{min}$ ) through the gel. For reference, an 11.5  $\mu\text{L}/\text{h}$  flow corresponds to a mean flow velocity of 10  $\mu\text{m}/\text{min}$ . Finally, cultures were maintained for 24 or 48 h according to the experiment.

*Interstitial flow application through HUVEC monolayers in cell culture inserts.* Culture of HUVECs on tissue culture inserts was developed as previously described.<sup>2</sup> Briefly, tissue culture inserts (12 mm diameter, 0.4  $\mu\text{m}$  pore size, catalog # PICM01250, Millicell-CM, Millipore, MA) were loaded with 200  $\mu\text{L}$  of melted agarose in water (0.5–2.5%). After the agarose solidified (20 min), 200  $\mu\text{L}$  of cold collagen I (liquid) at 2 mg/mL equilibrated in phosphate buffered saline (PBS) was loaded on top of the agarose gel. The inserts were placed into the cell culture incubator (37°C, 5%  $\text{CO}_2$ , in a humidified atmosphere) for 1 h to allow gelation. Next, collagen gels were equilibrated with EGM-2 without EGF or VEGF. When required, VEGF was added to the medium to a final concentration of 10 ng/mL. Sub-confluent ( $\sim 80,000$  cells/insert) or confluent ( $\sim 120,000$  cells/insert) cultures of HUVECs were seeded on top of the collagen gels. HUVEC monolayers were first cultured on top of the collagen gels as described above for 12 h. Then a column of 10 cm of medium (without VEGF or EGF) was applied on top by slipping a silicone tube (Silastic, Cole-Parmer, IL) over the edges of the tissue culture inserts and filling it with 10 cm of medium, producing a flow of medium through the HUVEC monolayer. An interstitial flow of approximately 50  $\mu\text{L}/\text{h}$ , corresponding to a mean flow velocity through the gel of approximately 10  $\mu\text{m}/\text{min}$ , comparable with the range observed within the vascular wall *in vivo*,<sup>23</sup> was obtained by applying a 2% agarose layer.

### EGFR pathway inhibition

No EGF or equivalent, such as heparin-binding EGF (HB-EGF), were added to the HUVEC culture medium formulation (EGM-2) in order to depend on the endogenous synthesis and release of the growth factor by the HUVECs, as previously described.<sup>3,31</sup> The inhibitors were added to the top medium of the device. We used Tyrphostin AG1478 (0.3  $\mu$ M, Catalog # T-4182, Sigma, St Louis, MO), which inhibits EGFR phosphorylation activation by EGF binding. The medium containing the inhibitor (and control without inhibitor) was replenished daily to ensure maintenance of the inhibitory activity.

### Fluorescence and immunostaining

**Detection of pSrc and BrdU-labeled cells.** Cells were fixed with 1% paraformaldehyde (PFA) in PBS for 2 h and then washed three times with PBS and incubated for 2 to 3 h at room temperature with blocking buffer (20% FBS, 1% dimethyl sulfoxide (DMSO) and 0.1% Triton X-100 in PBS). Then the samples were incubated with a rabbit anti-pSrc polyclonal antibody (Anti-Src [pY<sup>418</sup>], cat#44-660G, Biosource; Invitrogen, Carlsbad, CA) at a final concentration of 1  $\mu$ g/mL in blocking buffer for 2 h, washed three times with blocking buffer, incubated for 2 h with a rhodamine-conjugated donkey anti-rabbit IgG (catalog # SC 2095, Santa Cruz Biotechnology, Santa Cruz, CA) at a final concentration of 1  $\mu$ g/mL in blocking buffer, washed, and visualized under a fluorescent microscope. To detect proliferating cells BrdU was added for 6 h to the culture medium at a final concentration of 10  $\mu$ M when the interstitial fluid flow was applied. Then the samples were fixed with 1% PFA in PBS for 2 h and washed three times with PBS. Cells were then treated with 0.5 N hydrochloric acid in PBS for 30 min at 37°C, washed with PBS until reaching pH 7.4, and incubated for 2 to 3 h at room temperature with blocking buffer (20% FBS, 1% DMSO, and 0.1% Triton X-100 in PBS). Then samples were incubated with a fluorescein isothiocyanate-conjugated anti-BrdU mouse monoclonal antibody IgG (1:100 v/v dilution in the same blocking buffer; 556028, BD Biosciences). Fluorescent-positive cells were visualized with a Nikon TE300 microscope with phase contrast and epifluorescence capability. Images were acquired using a Hamamatsu camera (Hamamatsu Photonics, Bridgewater, NJ) using an Openlab data acquisition system (Improvision, Lexington, MA) and represent a single optical plane observed using phase contrast of fluorescence emission.

**Nuclei staining with DAPI.** DAPI staining was used to visualize the cells' nuclei. For this, cells were fixed with 4% PFA in PBS for 2 h. Then they were washed three times with PBS and incubated with DAPI (D-1306, Molecular Probes, Eugene, OR) diluted in PBS to a final concentration of 1  $\mu$ g/ $\mu$ L for 10 min. Finally the cells were washed three times with PBS and visualized using a Nikon TE300 microscope, and images were captured using a Hamamatsu camera with an Openlab data acquisition system.

**TRITC-phalloidin staining.** TRITC-phalloidin (77418, Fluka, St. Louis, MO) was used to stain the cells' actin fibers. Cells cultured inside the bioreactor were fixed with 4% PFA in PBS for 2 h and then washed 3 times with PBS. After this the cells were incubated at room temperature for 1 h with the TRITC-

phalloidin diluted in PBS (1:40 v/v). The cells were finally washed 3 times with PBS and visualized using a Nikon TE300 microscope. The images were captured with a Hamamatsu camera using an Openlab data acquisition system.

### Statistical analysis

Single optical planes were obtained using phase contrast of fluorescence emission of HUVECs cultured under each flow rate (velocities 2, 5, 10, 20, and 50  $\mu$ m/min). Image J 1.38x (National Institutes of Health, Bethesda, MD) software was used to analyze the images obtained. The number of clearly distinguishable capillary-like structures observed in each optical plane was determined, and capillary-like structures were measured to determine their length. Unpaired Student *t*-tests with  $\alpha=0.05$  were conducted to determine significant differences in capillary-like structure number and mean length between every possible pair of flows. Results are shown as means  $\pm$  standard errors of the mean.

## Results and Discussion

### Monolayer development and capillary-like structure formation

Endothelial cells were cultured for 48 h in the presence or absence of interstitial flow (11.5  $\mu$ L/h) (Fig. 1B). In the presence of interstitial flow, the endothelial monolayer was capable of forming numerous capillary-like structures with a wide range of lengths and number of cells. Most of the capillary-like structures that developed had branching, a feature of great relevance during the development of capillary-like structures *in vitro* (Fig. 1C). Moreover, this result indicates that the basic morphogenetic mechanism taking place in our new device was similar to the one previously reported.<sup>2</sup>

Previous experience had shown that neither interstitial flow nor VEGF alone was sufficient to promote a vascular morphogenic response in an endothelial monolayer but that the combination of the two factors had a clear synergistic effect on the formation of new capillary-like structures.<sup>2,32</sup> To confirm this synergism in our new bioreactor device, four experimental conditions were used: presence of VEGF with interstitial flow (at flow velocity  $\sim$ 10  $\mu$ m/min), presence of VEGF without interstitial flow, same intensity of interstitial flow in absence of VEGF, and no application of VEGF or flow. Results from these experiments confirmed our previous observations. In addition, they indicated that the mechanical stimulus exerted by the fluid flow operated similarly in our new device (Fig. 2A).

### Effect of flow intensity on capillary morphogenesis

To this point, we had confirmed the reproducibility of the basic parameters in our new device, including the capacity to generate capillary-like structures under the synergistic effect of interstitial flow and VEGF. Although interstitial flow is critical to initiating capillary morphogenesis, it is not real clear that the mechanical stimulus is important to maintain previously formed capillary-like structures. In addition, it was not determined previously whether an optimal flow rate (flow intensity) had an affect on the formation of capillary-like structures.

To determine whether the stimulus provided by flow was involved in the further development and maintenance of

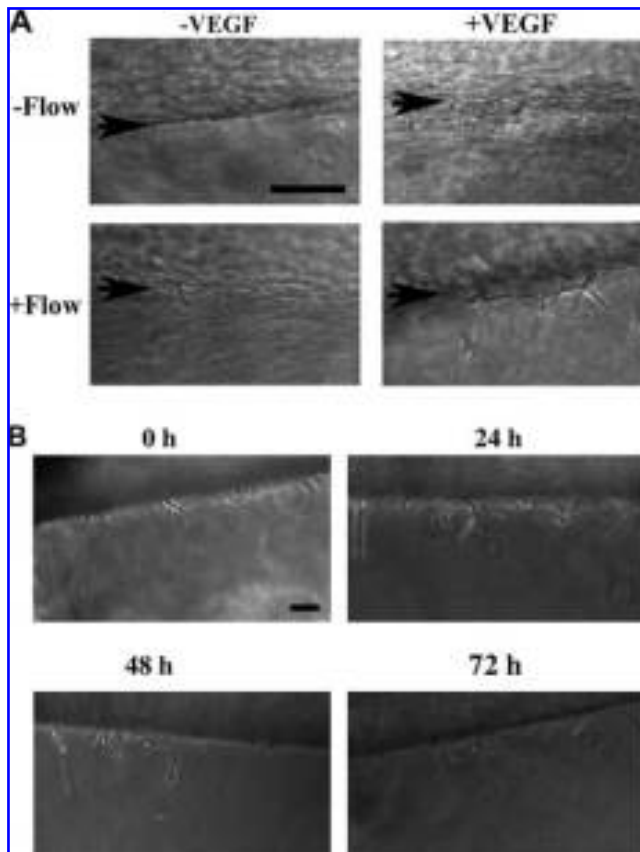


**FIG. 2.** Capillary-like structure progression and maintenance are dependent of vascular endothelial growth factor (VEGF) and interstitial flow. (A) To confirm the synergism of VEGF and interstitial flow in the new bioreactor device, four experimental conditions were used: VEGF with interstitial flow (at flow velocity  $\sim 10 \mu\text{m}/\text{min}$ ) (low-right panel), VEGF without interstitial flow (top-right panel), same intensity of interstitial flow in absence of VEGF (low-left panel), and no VEGF or flow (top-left panel). (B) Capillary-containing experiments were switched to conditions without flow to determine whether this absence caused any regression of the capillary-like structures formed during the overnight incubation period. Monitoring was performed every 24 h for a total 72 h. Interstitial flow removal led to a regression of the capillary-like structures in what appeared to be a multi-step process. First the branches originally observed (0 h) began to disappear, and the tips of the structures became rounded (24 h); then the capillaries lost their link to the monolayer, and single cells or fragments were seen inside the collagen gel (48 h); and finally, most of the capillary-like structures originally formed disintegrated completely (72 h). This shows that interstitial flow is necessary not only for the initiation of capillary-like structures, but also for their maintenance and further development. Black bar in top-left panels of A and B represents 200 and 100  $\mu\text{m}$ , respectively.

previously formed capillary-like structures, interstitial flow ( $11.5 \mu\text{L}/\text{h}$ ; corresponding to  $10 \mu\text{m}/\text{min}$ ) was applied overnight to pre-established HUVEC monolayers (obtained as previously described) to induce capillary-like structure formation. Then, these capillary-containing bioreactors were placed under no-flow conditions (Fig. 1B) and monitored every 24 h for a total of 72 h. The removal of interstitial flow

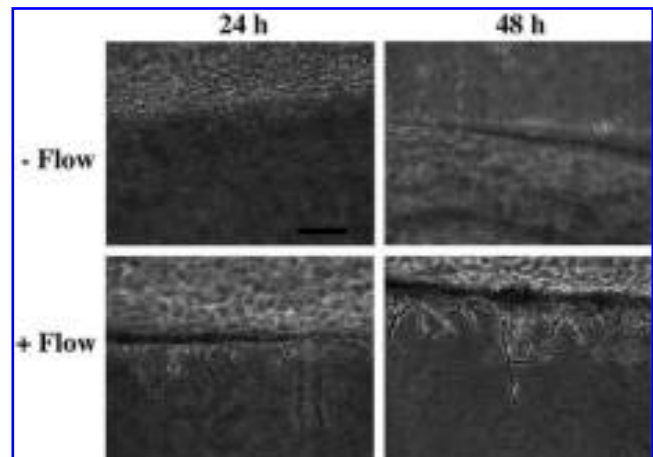


**FIG. 3.** Effect of interstitial flow in the promotion of the morphogenic response. Interstitial flow was applied to two bioreactors, for 24 and 48 h, respectively, and two static controls were cultured simultaneously to determine whether interstitial flow was a critical parameter for triggering the morphogenic response or if it contributed only to obtain a faster response from the monolayer. As expected, no morphogenic response was triggered after 24 h or 48 h (Fig. 4) in monolayers cultured in the absence of interstitial flow, therefore proving its key role in triggering the process of capillary morphogenesis. Black bar in top-left panel represents 100  $\mu\text{m}$ .

caused a regression of the capillary-like structures (Fig. 2B). This effect seemed to be a multi-step process in which first branches (Fig. 2B,  $t = 0 \text{ h}$ ) began to disappear, and the tips of the capillaries became rounded (Fig. 2B,  $t = 24 \text{ h}$ ); then the capillaries lost their link to the monolayer, and single cells or fragments were seen inside the collagen gel (Fig. 2B, 48 h); and finally, most of the capillary-like structures originally formed disappeared completely, suggesting the death of these cells or re-migration into the monolayer (Fig. 2B, 72 h). These results provide concluding evidence that the presence of interstitial flow is necessary not only for the initiation of capillary-like structures, but also for their maintenance and further development.

To study the effect of interstitial flow on capillary morphogenesis for a longer period of time, flow ( $11.5 \mu\text{L}/\text{h}$ ) was applied for 24 and 48 h (and static controls without flow). These experiments showed that, as expected, maintenance of the mechanical stimulus continued promoting capillary growth (Fig. 3).

Then, a new series of experiments aimed at studying the effect of different flow rates ( $0\text{--}50 \mu\text{m}/\text{min}$ ) in the morphogenic process was designed. The results showed that all of the flow rates led to the formation of capillary-like structures, supporting the previous observations that the presence of interstitial flow is critical to triggering the process (Fig. 4). However, differences between the structures formed in each case can be appreciated. Lower velocities (2 and  $5 \mu\text{m}/\text{min}$ , Fig. 4) led to small and simple capillaries with almost no branching; capillary-like structures formed under intermediate velocities (10 and  $20 \mu\text{m}/\text{min}$ ) showed longer length and greater complexity (most were branched, Fig. 4); and the highest velocity ( $50 \mu\text{m}/\text{min}$ ) induced the formation of some

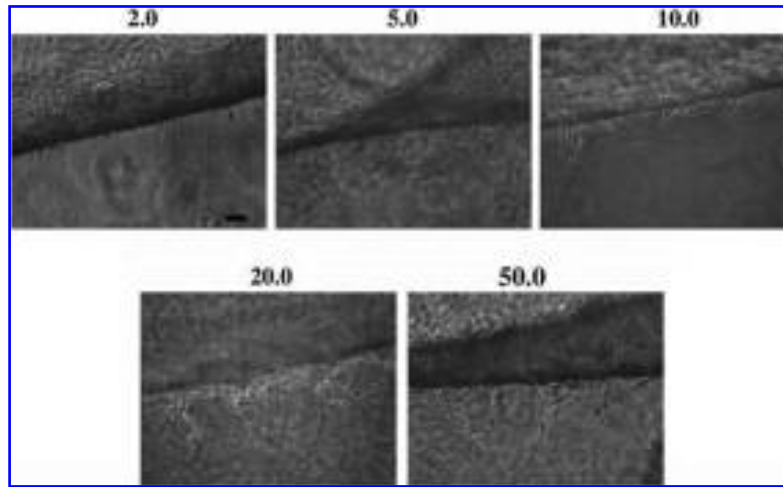


**FIG. 4.** Effect of flow rate in capillary-like structure formation. Five different flow rates (corresponding velocities: 2.0, 5.0, 10.0, 20.0, and 50.0  $\mu\text{m}/\text{min}$ ) were used to study the influence of flow rate in the formation of new capillary-like structures from a pre-established endothelial monolayer. All flow rates led to the formation of new structures, supporting the previous observations that interstitial flow is critical to triggering the process. However, some differences between the structures formed in each case can be appreciated. Lower velocities (2 and 5  $\mu\text{m}/\text{min}$ ) produced small and simple capillaries with almost no branching detected; intermediate velocities (10 and 20  $\mu\text{m}/\text{min}$ ) increased the length and complexity of the structures, and most had branches; and the highest velocity (50  $\mu\text{m}/\text{min}$ ) led to the formation of structures, but a significant disruption was observed, and single cells or fragments were often seen inside the collagen without any link to the monolayer. Therefore, velocities that presumably mimic the physiological conditions experienced by endothelial cells *in vivo* (10–20  $\mu\text{m}/\text{min}$ ) were optimal not only for the culture and maintenance of human umbilical vein endothelial cell monolayers, but also for the formation, growth, and development of new capillary-like structures. Black bar in top-left panel represents 100  $\mu\text{m}$ .

structures, but a significant disruption was observed, and single cells were often seen inside the collagen without any link to the monolayer (Fig. 4). These results confirm that velocities of 10 to 20  $\mu\text{m}/\text{min}$ , which presumably mimic the physiological conditions experienced by endothelial cells *in vivo*,<sup>23</sup> are optimal not only for the culture and maintenance of HUVEC monolayers,<sup>2</sup> but also for the formation, growth, and development of new capillary-like structures (Fig. 4).

Interstitial flow rate promotes capillary growth rather than capillary number.

To determine whether interstitial flow rate was affecting mainly capillary growth, number, or both, a further analysis regarding the effect of flow rate in the number of initial capillary-like structures formed, the number of branches observed, and the average length of the new structures was performed.

First, we noticed that fluid flow was required to induce the morphogenic process but that flow intensity played no apparent role in modulating the average number of new capillary-like structures formed, because no significant differences were observed between the different flow rates tested ( $p > 0.05$  for each pair of flows; Fig. 5A). This might imply that there are a pre-determined number of “initiation zones” on the cell monolayer that will undergo morphogenesis under the synergistic effect of interstitial flow (at least for rates of  $\sim 0$ –50  $\mu\text{m}/\text{min}$ ) and VEGF. Instead, flow intensity seems to influence capillary length, showing a maximum at flow velocities of 10 and 20  $\mu\text{m}/\text{min}$  (Fig. 5B). Significant differences in length were observed between the lowest velocity (2  $\mu\text{m}/\text{min}$ ) and the rest ( $p < 0.005$  in every case) and between 5 and 20  $\mu\text{m}/\text{min}$  ( $p = 0.008$ ). A nearly significant difference was observed between 5 and 20  $\mu\text{m}/\text{min}$ . Although no significant differences were ob-

served between 10, 20, and 50  $\mu\text{m}/\text{min}$  ( $p > 0.05$  in each case; Fig. 5B), the difference in branching observed when comparing the structures formed under 10 and 20  $\mu\text{m}/\text{min}$  with those formed at 50  $\mu\text{m}/\text{min}$  must be highlighted.

Flow rates corresponding to 10- and 20- $\mu\text{m}/\text{min}$  velocities have been proven to increase cell proliferation within the monolayer,<sup>2</sup> therefore increasing the number of cells capable of migrating into the surrounding matrix to form longer and more-complex capillary-like structures. This is in accordance with the idea that, to increase the length of a capillary-like structure, it is necessary to increase the production of cells by increasing proliferation at the monolayer.<sup>2</sup> Nevertheless, the effect that flow exerts on monolayer growth alone cannot explain the observation that fluid flow modulates capillary growth but not the average number of capillaries. Instead, some intrinsic property of the monolayer must control capillary number. For this reason, we decided to analyze the distribution of the activated (phosphorylated) form of Src (pSrc), an intermediate player in mechanosignal transduction.<sup>30,33–36</sup>

#### *Interstitial flow intensity modulates sprouting only in Src-activated cell clusters*

Mechanical stimuli activate integrins<sup>35</sup> (a family of transmembrane adhesion receptors that mediate cellular adhesion and motility on extracellular matrix molecules)<sup>37</sup> and the cytoskeleton to regulate cellular functions such as movement, adhesion, and eventually morphogenesis. When activated, integrins associate to the Src tyrosine kinase (a component of focal adhesion complexes) via its SH<sub>3</sub> domain, unmasking the kinase domain and leading to a stable activation of Src by autophosphorylation on residue Tyr-

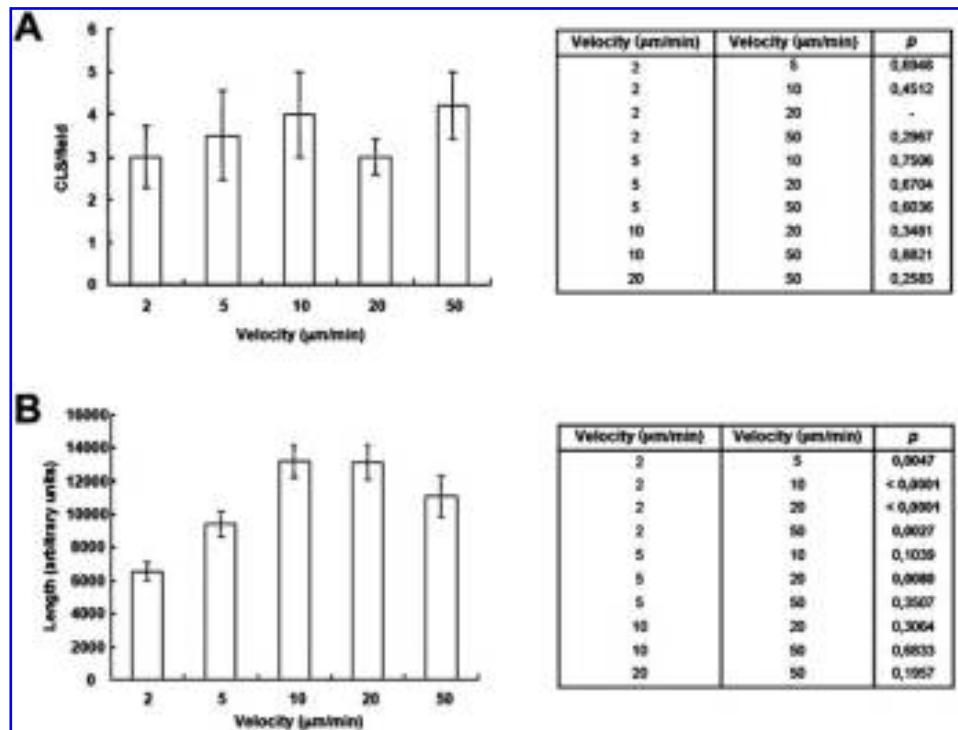


**FIG. 5.** Effect of flow rate on number and length of capillary-like structures. **(A)** Results obtained with the application of five different flow rates (Fig. 4) were analyzed to determine the influence of flow rate on the total number of clearly distinguishable capillary-like structures in each optical plane. Flow rate had no significant effect in the average number of capillary-like structures formed ( $p > 0.05$  for every pair of flows), indicating that flow is required to initiate the morphogenetic process but has no apparent participation in modulating the amount of formed capillary-like structures. (See table at the right of graphic A.) **(B)** Flow rates that presumably mimic physiological conditions (10–20  $\mu\text{m}/\text{min}$ ) have been proven to increase cell proliferation through the monolayer and therefore increase the number of cells capable of migrating into the surrounding matrix.<sup>2</sup> Accordingly, this flow rate led to the formation of significantly longer capillary-like structures. (See statistically significant differences in table at the right of graphic B.) Number of structures measured for each flow velocity: 2  $\mu\text{m}/\text{min}$ , 18; 5  $\mu\text{m}/\text{min}$ , 14; 10  $\mu\text{m}/\text{min}$ , 12; 20  $\mu\text{m}/\text{min}$ , 12; 50  $\mu\text{m}/\text{min}$ , 21. Results are shown as means  $\pm$  standard errors of the mean.

418.<sup>27,30</sup> For this reason, we decided to use 4-amino-5-(4-chlorophenyl)-7-(*t*-butyl)pyrazolo[3,4-*d*]pyrimidine (PP2; 529573, Calbiochem, San Diego, CA), a potent and selective inhibitor of the Src family of protein tyrosine kinases,<sup>28</sup> to study its effect on the formation of new capillary-like structures. HUVECs were induced to produce capillary-like structures in the bioreactors at a constant flow of 11.5  $\mu\text{L}/\text{h}$  (equivalent to a flow velocity of 10  $\mu\text{m}/\text{min}$ ) for 24 h in the presence or absence of 10  $\mu\text{M}$  of PP2.

Using visual inspection of the structures formed in control experiments and comparing them with those treated with PP2, it becomes evident that, when Src phosphorylation was inhibited, only a few single cells were observed migrating inside the collagen disconnected from the monolayer (Fig. 6A). A significant difference in capillary-like structures per optical plane in cells treated with and without PP2 was observed (0.66 vs  $3.33 \pm 0.33$ ;  $p < 0.002$ ) (Fig. 6A).

The disruption on the morphogenic response caused by the inhibition of Src activation by PP2 gave us some evidence of the role of this tyrosine kinase (key component of the mechanotransduction pathway<sup>33–35,38</sup>) in the process of capillary morphogenesis in our system. Based on this result, we analyzed whether interstitial flow rate modulates the level of Src activation at the cell membrane. For this purpose, we compared, using Western blot, the relative amounts of

total Src and phosphorylated Src (pSrc) present in cells cultured for 24 h under six different flow conditions: no interstitial flow and five different flow rates (2.3, 5.7, 11.5, 23.0, and 57.4  $\mu\text{L}/\text{h}$ , corresponding to mean flow velocities through the chamber of 2, 5, 10, 20, and 50  $\mu\text{m}/\text{min}$ , respectively). The ratio of pSrc to total Src protein, both normalized with actin, showed a maximum at flow velocities of 10 and 20  $\mu\text{m}/\text{min}$  (Fig. 6C). Although this experiment was performed twice, and no statistical data were obtained, this could suggest an explanation of why those flow rates had proven to be optimal for HUVEC monolayer establishment as well as for the development and maintenance of new capillary-like structures (see above).

Next we were interested in visualizing the distribution of pSrc on the endothelial monolayer under interstitial flow conditions as well as in controls. Hence, we performed immunostaining using a specific antibody against pSrc (see Materials and Methods). We detected that the monolayer was not uniformly stained for pSrc; instead, distinct patches of cells containing pSrc (localized at the periphery of the cells) were surrounded by non-pSrc cells (Fig. 7A, B). This clearly suggested that a heterogenic distribution of mechanically activated cell clusters could be the cause of having a predetermined number of “capillary initiation sites.” Capillary-like structures developed only from zones where

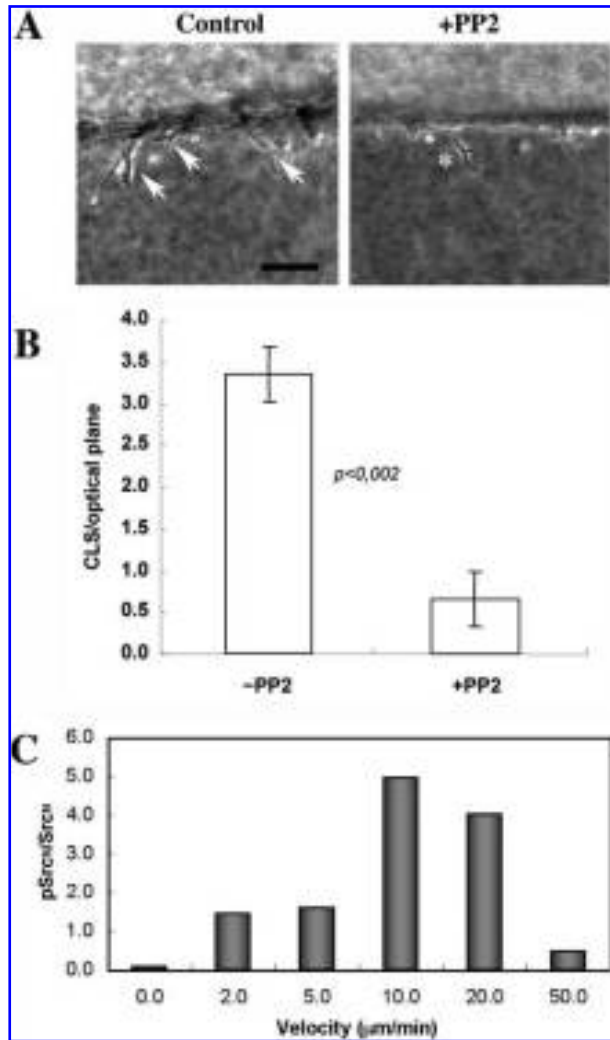


**FIG. 6.** Effect of Src inhibition on capillary-like structure formation. (A) When 4-amino-5-(4-chlorophenyl)-7-(*t*-butyl) pyrazolo[3,4-*d*]pyrimidine (PP2, a potent and selective inhibitor of the Src family of protein tyrosine kinases) was incorporated into the medium, a few small, non-branched structures were formed, and single cells or fragments could be seen inside the collagen (\*). Controls showed a greater number of more-complex structures (arrows). Black bar at left panel represents 100  $\mu\text{m}$ . (B) PP2 significantly decreased the number of capillary-structures observed ( $p > 0.002$ ). (C) Src and phosphorylated Src (pSrc) levels were analyzed using Western blot. The ratio of normalized pSrc (pSrc/actin) to normalized Src (Src/actin) showed significantly more Src phosphorylation in samples taken from cells cultured without flow (pSrc<sub>N</sub>/Src<sub>N</sub>  $\sim 0$ ) than in those where interstitial flow was applied. Phosphorylation levels showed a peak at flows previously found to be optimal for human umbilical vein endothelial cell monolayer culture and maintenance, as well as for the formation, growth, and development of new capillary-like structures (10.0–20.0  $\mu\text{m}/\text{min}$ ).

Src was highly activated (pSrc zones) (Fig. 7A–D). In other words, the monolayer could dictate which cells would undergo capillary morphogenesis and which ones would not. If this is the case, is the establishment of pSrc zones in monolayers pre-determined, or does the mechanical stimulus

of interstitial fluid flow generate it? To answer this question, we immunostained monolayers for pSrc obtained with or without interstitial flow and found that the pattern of pSrc patches surrounded by non-pSrc cells was present regardless of flow stress, thus indicating that it might be an intrinsic property of the endothelial monolayer system under the experimental condition tested (Fig. 8B). The different levels of pSrc found with varying flow rates must therefore indicate variations in the level of activation or number of activated cells within the same number of activated sites.

Moreover, we tested the effect of the presence or absence of FGFb, as well as the EGFR inhibitor (AG1478) to see whether these agents regulate in some way the pattern of activated and non-activated Src patches. We found that the absence of FGFb or the inhibition of EGFR reduced the number of non-pSrc cells in each patch, suggesting that FGFb and the EGFR pathway regulate the presence of mechanically non-activated zones (Fig. 8). It is exciting because we know, from previous results, that FGFb and the EGFR pathway are essential players in capillary morphogenesis, because their absence or inhibition affects the process.<sup>2</sup> Therefore, this result suggests that those mechanically non-activated zones are essential in engaging pSrc cells in undergoing morphogenesis. In view of these results, we suggest that FGFb or the EGFR pathway controls the maintenance of non-mechanically activated zones, restricting the number and distance of pSrc areas in the monolayer. In addition, the presence of non-pSrc zones could be important in fostering cell proliferation, because environmental factors could control cell division: therefore, areas of non-mechanically engaged cells could be optimal regions for cell division. In contrast, migratorily active pSrc areas undergoing capillary morphogenesis could promote cell cycle arrest. For this reason, we incubated HUVEC monolayers for 6 h under interstitial flow conditions with BrdU (to detect dividing cells at the S-phase), followed by double immunostaining for BrdU and pSrc (see Materials and Methods). BrdU<sup>+</sup> cells were detected in pSrc as well as non-pSrc zones but not in sprouting cells, indicating that a cell might be “mechanically sensitive” (pSrc) and still be able to proliferate unless it is strictly engaged in morphogenesis and actively committed to the development of a capillary structure (Fig. 9). This suggests that FGFb and the EGFR pathway control in part the mechanism in charge of controlling the distribution of pSrc zones and cell proliferation restricted to the monolayer, but extensive research needs to be done to understand this process clearly.

## Conclusions

In the present work, we observed that interstitial flow intensity affects the length and branching degree but not the number of capillary-like structures developed from HUVEC monolayers and that capillary morphogenesis is restricted to patches of Src-activated cells (pSrc) at the cell monolayer. Specifically, we found that the length and branching degree of the capillary-like structures was maximum at flow values of 10 to 20  $\mu\text{m}/\text{min}$ . This suggests that the endothelial monolayer presents predetermined areas of “capillary initiation spots” that remain unchanged across the flow velocities tested (2–50  $\mu\text{m}/\text{min}$ ). Additionally, the phosphorylation state of Src (a component of focal adhesion complexes) across the mono-

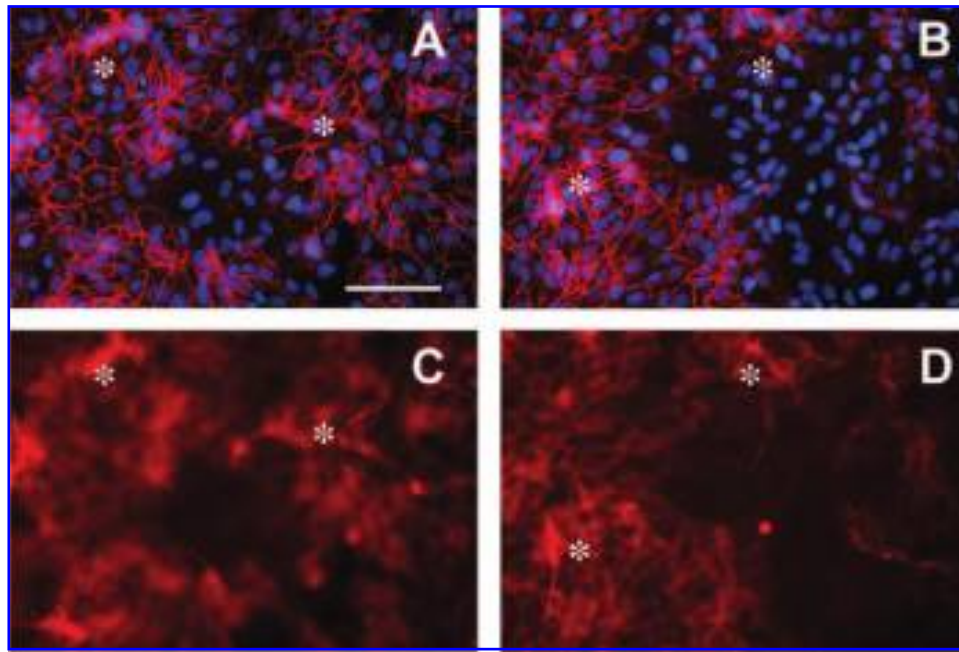


**FIG. 7.** Strictly Src-activated (pSrc) clusters of human umbilical vein endothelial cells (HUVECs) undergo capillary morphogenesis. Cells under interstitial flow of  $10.0 \mu\text{m}/\text{min}$  were fixed and immunostained for pSrc. Defined zones or clusters of pSrc HUVECs can be visualized (red) at the monolayer (**A, B**). White asterisks indicate zones of highly activated pSrc in the monolayer. Underneath the monolayer ( $10\text{--}20 \mu\text{m}$ ), capillary-like structures positive for pSrc immunostaining can be visualized, all emerging from pSrc zones of the monolayer (**C, D**). For reference, the white asterisks indicate the same zones in panels (**A**) and (**B**). Nuclei were stained with 4',6-diamidino-2-phenylindole, dihydrochloride (blue). White bar in **A** represents  $100 \mu\text{m}$ . Color images available online at [www.liebertpub.com/ten](http://www.liebertpub.com/ten).

layer presented a heterogeneous distribution, showing distinct phosphorylated Src (pSrc) cell clusters surrounded by non-phosphorylated Src (non-pSrc) cells. Moreover, all new capillary-like structures emerged from pSrc zones, indicating

that predetermined Src-activated areas (pSrc) are the only restricted zones to undergo capillary morphogenesis and that the number of these is independent of interstitial flow. In summary, endothelial monolayers cultured under the conditions

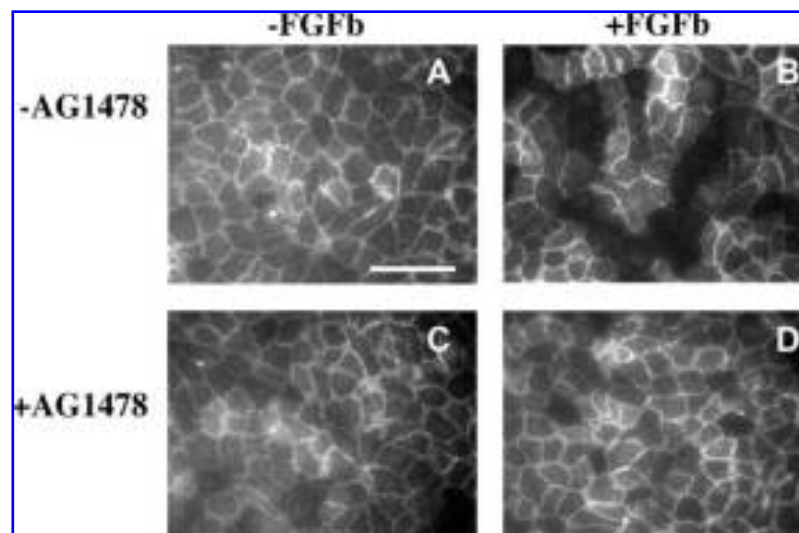


**FIG. 8.** Basic fibroblast growth factor (FGFb) and the endothelial growth factor receptor (EGFR) pathway regulate non-activated Src zone sizes. Human umbilical vein endothelial cell (HUVEC) monolayers were cultured without interstitial flow conditions, combining the presence or absence of FGFb and the EGFR pathway inhibitor AG1478. (**A**) Cells cultured in the absence of FGFb and AG1478, (**B**) in the presence of FGFb and the absence of AG1478 (controls), (**C**) in the absence of FGFb and the presence of AG1478, and (**D**) the presence of FGFb and AG1478. Only the absence of FGFb or the presence of AG1478 alone, or both conditions together, decreased dramatically the cell number of non-activated Src clusters. White bar in **A** represents  $100 \mu\text{m}$ .

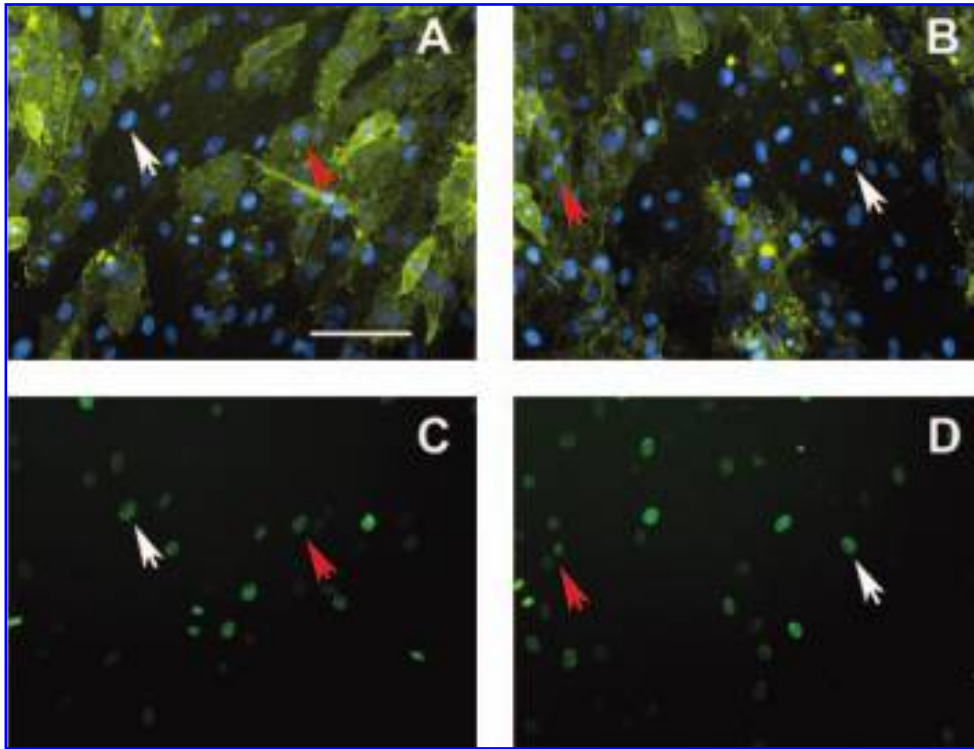


**FIG. 9.** Activated and non-activated Src cells undergo cell proliferation. Human umbilical vein endothelial cell (HUVEC) monolayers cultured under interstitial flow (10  $\mu\text{m}/\text{min}$ ) were incubated for 6 h in the presence of 5'-bromo-2'-deoxyuridine (BrdU, 10  $\mu\text{M}$ ), fixed and immunostained for BrdU and pSrc (see Materials and Methods). HUVECs stained for pSrc (yellow) and for nuclei with 4',6-diamidino-2-phenylindole, dihydrochloride (blue) (A, B) were also stained for BrdU (green). The same optical layer of panel A corresponds to panel C and B to D. White arrows indicated BrdU<sup>+</sup> nuclei in non-activated Src cells; red arrows indicate nuclei in activated Src cells (pSrc). White bar in A represents 100  $\mu\text{m}$ . Color images available online at [www.liebertpub.com/ten](http://www.liebertpub.com/ten).

tested present a predetermined distribution of mechanically sensitive zones (pSrc) that engage in capillary morphogenesis under the right biomechanical stimuli, promoting cell proliferation at the monolayer and cell migration and therefore capillary growth.

Although in our present work we used HUVECs, it seems logical to extend this study to other endothelial systems, including human microvascular vein endothelial cells and human microvascular endothelial cells, which have phenotypes much more similar to those of the *in vivo* capillary sprouting systems found in tissues and organs. Therefore, these endothelial systems could be employed to develop vascular networks *in vitro* for direct tissue engineering applications in areas such as production of skin analogs and artificial organ constructs. The cells could be easily isolated from patients and used to develop tissue constructs for autologous applications, avoiding future complications with the immune system. Moreover, the addition of pericyte-like cells would allow the stabilization of these networks because the intimate interaction between pericytes and endothelial cells maintains the vascular architecture within tissues.

#### Acknowledgments

We are grateful to discussions with and useful advice from Cherry Wan, Vernella Vickerman, and Francisco Carrión. This study was supported in part by a Draper Laboratories

Research grant and National Institutes of Health research grant 1-RO1-EB003805-01A1 to RK and CES, and award 1098SF TRM, Leipzig University, Germany, to CES.

#### References

1. Vogel, V., and Baneyx, G. The tissue engineering puzzle: a molecular perspective. *Annu Rev Biomed Eng* **5**, 441, 2003.
2. Semino, C.E., Kamm, R.D., and Lauffenburger, D.A. Autocrine EGF receptor activation mediates endothelial cell migration and vascular morphogenesis induced by VEGF under interstitial flow. *Exp Cell Res* **312**, 289, 2006.
3. Arkonac, B.M., Foster, L.C., Sibinga, N.E.S., Patterson, C., Lai, K., Tsai, J.-C., Lee, M.-E., Perella, M.A., and Haber, E. Vascular endothelial growth factor induces heparin-binding epidermal growth factor-like growth factor in vascular endothelial cells. *J Biol Chem* **273**, 4400, 1998.
4. Cross, M.J., and Claesson-Welsh, L. FGF and VEGF function in angiogenesis: signalling pathways, biological responses and therapeutic inhibition. *Trends Pharmacol Sci* **22**, 201, 2001.
5. Debabrata, M., Huiyan, Z., and Resham, B. Complexity in the vascular permeability factor/vascular endothelial growth factor (VPF/VEGF)-receptors signaling. *Molec Cell Biochem* **264**, 51, 2005.
6. Ferrara, N. VEGF and the quest for tumour angiogenesis factors. *Nat Rev Cancer* **2**, 795, 2002.
7. Ferrara, N., Gerber, H.-P., and LeCouter, J. The biology of VEGF and its receptors. *Nat Med* **9**, 669, 2003.

8. Sipos, B., Weber, D., Ungefroren, H., Kalthoff, H., Zühlsdorff, A., Luther, C., Török, V., and Klöppel, G. Vascular endothelial growth factor mediated angiogenic potential of pancreatic ductal carcinomas enhanced by hypoxia: An *in vitro* and *in vivo* study. *Int J Cancer* **102**, 592, 2002.
9. Yancopoulos, G.D., Davis, S., Gale, N.W., Rudge, J.S., Wiegand, S.J., and Holash, J. Vascular-specific growth factors and blood vessel formation. *Nature* **407**, 242, 2000.
10. Zachary, I. VEGF signalling: integration and multi-tasking in endothelial cell biology. *Biochem Soc Trans* **31**, 1171, 2003.
11. Hoffmann, S., Gläser, S., Wunderlich, A., Lingelbach, S., Dietrich, C., Burchert, A., Müller, H., Rothmund, M., and Zielke, A. Targeting the EGF/VEGF-R system by tyrosine-kinase inhibitors—a novel antiproliferative/antiangiogenic strategy in thyroid cancer. *Langenbecks Arch Surg* **391**, 589, 2006.
12. van Cruijssen, H., Giaccone, G., and Hoekman, K. Epidermal growth factor receptor and angiogenesis: opportunities for combined anticancer strategies. *Int J Cancer* **117**, 883, 2005.
13. Rusnati, M., and Presta, M. Fibroblast growth factors/fibroblast growth factor receptors as targets for the development of anti-angiogenesis strategies. *Curr Pharm Des* **13**, 2025, 2007.
14. Shibuya, M. Nucleotide sequence and expression of a novel human receptor-type tyrosine kinase gene (flt) closely related to the fms family. *Oncogene* **5**, 519, 1990.
15. Guo, D., Jia, Q., Song, H.-Y., Warren, R.S., and Donner, D.B. Vascular endothelial cell growth factor promotes tyrosine phosphorylation of mediators of signal transduction that contain SH2 domains. *J Biol Chem* **270**, 6729, 1995.
16. Boardman, K.C., and Swartz, M.A. Interstitial flow as a guide for lymphangiogenesis. *Circ Res* **92**, 801, 2003.
17. Ng, C.P., Helm, C.-L.E., and Swartz, M.A. Interstitial flow differentially stimulates blood and lymphatic endothelial cell morphogenesis *in vitro*. *Microvasc Res* **68**, 258, 2004.
18. Ng, C.P., and Swartz, M.A. Fibroblast alignment under interstitial fluid flow using a novel 3-D tissue culture model. *Am J Physiol Heart Circ Physiol* **284**, H1771, 2003.
19. Rutkowski, J.M., and Swartz, M.A. A driving force for change: interstitial flow as a morphoregulator. *Trends Cell Biol* **17**, 44, 2007.
20. Swartz, M.A., and Boardman, K.C., Jr. The role of interstitial stress in lymphatic function and lymphangiogenesis. *Ann N Y Acad Sci* **979**, 197, 2002.
21. Swartz, M.A. Signaling in morphogenesis: transport cues in morphogenesis. *Curr Opin Biotechnol* **14**, 547, 2003.
22. Helm, C.-L.E., Zisch, A., and Swartz, M.A. Engineered blood and lymphatic capillaries in 3-D VEGF-fibrin-collagen matrices with interstitial flow. *Biotechnol Bioeng* **96**, 167, 2007.
23. Chary, S.R., and Jain, R.K. Direct measurement of interstitial convection and diffusion of albumin in normal and neoplastic tissues by fluorescence photobleaching. *Proc Natl Acad Sci USA* **86**, 5385, 1989.
24. Bayless, K.J., and Davis, G.E. Sphingosine-1-phosphate markedly induces matrix metalloproteinase and integrin-dependent human endothelial cell invasion and lumen formation in three-dimensional collagen and fibrin matrices. *Biochem Biophys Res Commun* **312**, 903, 2003.
25. Davis, G.E., and Camarillo, C.W. An  $[\alpha]_2[\beta]_1$  integrin-dependent pinocytic mechanism involving intracellular vacuole formation and coalescence regulates capillary lumen and tube formation in three-dimensional collagen matrix. *Exp Cell Res* **224**, 39, 1996.
26. Yang, S., Graham, J., Kahn, J.W., Schwartz, E.A., and Gertsen, M.E. Functional roles for PECAM-1 (CD31) and VE-cadherin (CD144) in tube assembly and lumen formation in three-dimensional collagen gels. *Am J Pathol* **155**, 887, 1999.
27. Arias-Salgado, E.G., Lizano, S., Sarkar, S., Brugge, J.S., Ginsberg, M.H., and Shattil, S.J. Src kinase activation by direct interaction with the integrin  $\beta$  cytoplasmic domain. *Proc Natl Acad Sci USA* **100**, 13298, 2003.
28. Kilariski, W.W., Jura, N., and Gerwins, P. Inactivation of Src family kinases inhibits angiogenesis *in vivo*: implications for a mechanism involving organization of the actin cytoskeleton. *Exp Cell Res* **291**, 70, 2003.
29. Liu, Y., and Senger, D.R. Matrix-specific activation of Src and Rho initiates capillary morphogenesis of endothelial cells. *J Fed Am Soc Exper Biol* **18**, 457, 2004.
30. Wang, Y., Botvinick, E.L., Zhao, Y., Berns, M.W., Usami, S., Tsien, R.Y., and Chien, S. Visualizing the mechanical activation of Src. *Nature* **434**, 1040, 2005.
31. Morita, T., Yoshizumi, M., Kurihara, H., Maemura, K., Nagai, R., and Yazaki, Y. Shear stress increases heparin-binding epidermal growth factor-like growth factor mRNA levels in human vascular endothelial cells. *Biochem Biophys Res Commun* **197**, 256, 1993.
32. Helm, C.-L.E., Fleury, M.E., Zisch, A.H., Boschetti, F., and Swartz, M.A. Synergy between interstitial flow and VEGF directs capillary morphogenesis *in vitro* through a gradient amplification mechanism. *Proc Natl Acad Sci* **102**, 15779, 2005.
33. Chien, S. Mechanotransduction and endothelial cell homeostasis: the wisdom of the cell. *Am J Physiol Heart Circ Physiol* **292**, H1209, 2007.
34. Huang, H., Kamm, R.D., and Lee, R.T. Cell mechanics and mechanotransduction: pathways, probes, and physiology. *Am J Physiol Cell Physiol* **287**, C1, 2004.
35. Katsumi, A., Orr, A.W., Tzima, E., and Schwartz, M.A. Integrins in mechanotransduction. *J Biol Chem* **279**, 12001, 2004.
36. Tzima, E., Irani-Tehrani, M., Kiosses, W.B., Dejana, E., Schultz, D.A., Engelhardt, B., Cao, G., DeLisser, H., and Schwartz, M.A. A mechanosensory complex that mediates the endothelial cell response to fluid shear stress. *Nature* **437**, 426, 2005.
37. Felsenfeld, D.P., Schwartzberg, P.L., Venegas, A., Tse, R., and Sheetz, M.P. Selective regulation of integrin-cytoskeleton interactions by the tyrosine kinase Src. *Nat Cell Biol* **1**, 200, 1999.
38. Li, S., Huang, N.F., and Hsu, S. Mechanotransduction in endothelial cell migration. *J Cell Biochem* **96**, 1110, 2005.

Address reprint requests to:  
 Carlos E. Semino, Ph.D.  
 77 Massachusetts Avenue  
 Building NE-47 Room 383  
 Cambridge, MA 02139

E-mail: semino@mit.edu

Received: September 28, 2007

Accepted: May 5, 2008